ANTICANCER RESEARCH *38*: 1927-1935 (2018)
doi:10.21873/anticanres.12430

Differential Organ-targeting and Cellular Characteristics of Metastatic Human Pancreatic Cancer Cell Lines in Mouse Models

TOMOYUKI SATAKE[1], ATSUSHI SUETSUGU[1,2,3], MIKI NAKAMURA[1], KOSUKE HASEGAWA[1], TAKAHIRO KUNISADA[1], MASAHITO SHIMIZU[1], SHIGETOYO SAJI[1], HISATAKA MORIWAKI[1] and ROBERT M. HOFFMAN[2,3]

[1]*Gifu University Graduate School of Medicine, Gifu, Japan;*
[2]*AntiCancer, Inc. San Diego, CA, U.S.A.;*
[3]*Department of Surgery, University of California, San Diego, CA, U.S.A.*

Abstract. *Background/Aim: The lethal characteristic of pancreatic cancer is metastasis which is recalcitrant to currently-used chemotherapy. Our aim was to understand metastasis at the cellular level. We previously reported that multi-nucleate cells or spindle cells were more prominent in pancreatic cancer metastasis than in the primary tumor. In the present report, we investigated four representative human pancreatic cell lines for differences in cell morphology between the primary tumor and various metastatic organ targets for each cell line. Materials and Methods: Human pancreatic cancer cell lines AsPC-1, Panc-1, KP2 and KP3 were used. Pancreatic cancer cells were injected into spleen of nude mice resulting in experimental metastasis to various organs which were observed at the cellular level when the organs were placed into culture. Results: AsPC-1 and KP2 pancreatic cells formed many experimental liver metastases, in contrast to Panc-1 and KP3. Lung metastasis was only observed for AsPC-1. In the cultures established from the primary and metastatic tumors, multi-nucleate cells were found to be more prominent in the metastasis of the pancreatic cell lines with frequent metastasis, AsPC-1 and KP2. Spindle-like cells were observed prominently in AsPC-1 lung metastasis. Conclusion: Human pancreatic cancer cell lines have differential metastatic characteristics with regard to target organs and cell-morphology changes. Multi-nucleate and spindle cells may play an important role in pancreatic cancer metastasis to the liver and lung, respectively.*

Correspondence to: Atsushi Suetsugu, MD, Ph.D., Department of Gastroenterology, Gifu University Graduate School of Medicine, 1-1 Yanagido, Gifu 501-1194, Japan. Tel: +81 582306308, Fax: +81 582306310, e-mail: asue@gifu-u.ac.jp; or Robert M. Hoffman, Ph.D., Anti Cancer, Inc., 7917 Ostrow Street, San Diego, CA 92111, U.S.A. Tel: +1 8586542555, Fax: +1 8582684175, e-mail: all@anticancer.com

Key Words: Pancreatic cancer, niche, liver metastasis, multinucleate cells, spindle cells, green fluorescent protein.

Pancreatic cancer is among the most recalcitrant of all malignancies (1, 2). The lethal characteristic of pancreatic cancer is metastasis (3-6). Our laboratory pioneered the use of green fluorescent protein (GFP) to visualize metastatic cancer cells *in vivo* in live mouse models (7-11). GFP- and red fluorescent protein (RFP)-labeled cancer and stromal cells allowed us to pioneer color-coded imaging of the tumor microenvironment (TME) of pancreatic cancer (12-20).

Using GFP imaging, we previously showed that multi-nucleated pancreatic cancer cells were related to peritoneal metastasis of pancreatic cancer in mouse models (21). We also previously showed, using GFP imaging technology, that spindle cells were more aggressive than round cells in a dimorphic human pancreatic cancer cell line, in mouse models (22). An epithelial to mesenchymal transition (EMT) may have a role in metastasis development, whereby the cancer cells acquire spindle-like morphology (23-30).

In the present study, using human pancreatic cancer cell lines brightly expressing GFP, we investigated the presence of multi-nucleate and spindle cells cultured from the pancreatic metastasis to different organs in nude mice to determine their role in the metastatic process.

Materials and Methods

Mice. Six-week BALB/C athymic *nu/nu* female nude mice (Charles River Laboratories Inc., Yokohama, Japan), 4-6 weeks old, were used in this study. In order to minimize any suffering of the animals, anesthesia and analgesics were used for all surgical experiments. Animals were anesthetized by subcutaneous injection of a 0.02 ml solution of 20 mg/kg ketamine. The response of animals during surgery was monitored to ensure adequate depth of anesthesia. The

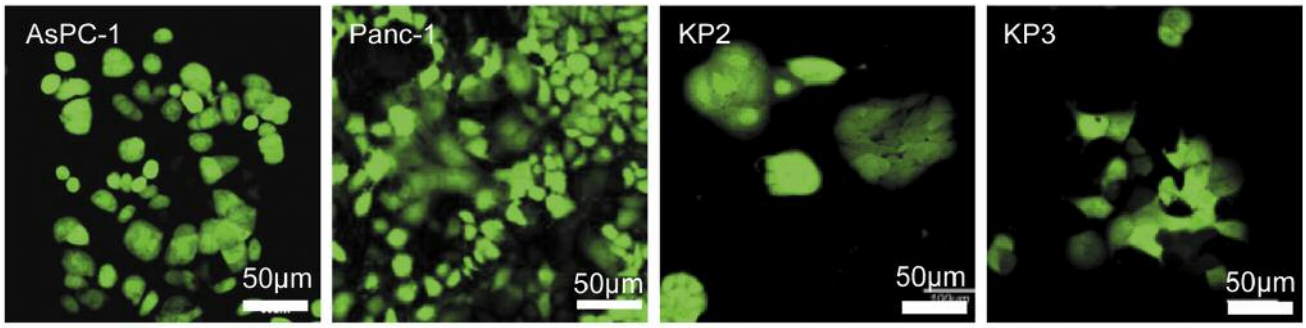

Figure 1. *Fluorescence images of pancreatic cancer cell lines expressing green fluorescent protein (GFP). Images were obtained with the Olympus FV1000 confocal microscope.*

animals were observed on a daily basis and sacrificed by CO_2 inhalation when they met the following humane endpoint criteria: severe tumor burden (more than 20 mm in diameter), prostration, significant body weight loss, difficulty breathing, rotational motion and body temperature drop. Animals were housed in a barrier facility on a high efficiency particulate arrestance (HEPA)-filtered rack under standard conditions of 12-hour light/dark cycles. The animals were fed an autoclaved laboratory rodent diet (31).

Study approval. All experiments were conducted in accordance with the Institutional Guidelines of Gifu University and were approved by the Animal Research Committee and the Committee on Living Modified Organisms of Gifu University.

Cell lines and culture conditions. AsPC-1, Panc-1, KP2, and KP3 human pancreatic cancer cells, were all engineered to stably express green fluorescent protein (GFP) using previously reported methodology (9-11, 32-34). The cells were maintained in RPMI 1640 medium (GIBCO-BRL, Grand Island, NY, USA) supplemented with 10% heat-inactivated fetal bovine serum (FBS) and 1% penicillin and streptomycin (GIBCO-BRL). The cells were cultured in a humidified atmosphere containing 5% CO_2 at 37˚C.

Pancreatic cancer experimental metastatic model. Six-week-old nude mice were used as hosts. Pancreatic cancer cells were harvested from culture by trypsinization and washed three times with cold serum-free medium, then re-suspended in serum-free RPMI 1640 medium. Each cell line (2.0×10^6 cells) was injected in the spleen of male mice. After six weeks, mice were sacrificed and the primary tumor and metastatic tumors were harvested. The cells from primary tumor and metastatic tumors were cultured for several weeks.

Imaging. The SZX7 microscope and FV1000 confocal microscope (Olympus Corp. Tokyo, Japan) were used for imaging.

Histology. Tumors were pathologically confirmed by using hematoxylin and eosin (H&E) staining. Fresh tumor samples were fixed in 10% formalin and embedded in paraffin before sectioning and staining. Tissue sections (5 μm) were deparaffinized in xylene and rehydrated in an ethanol series. Hematoxylin and eosin (H&E) staining was performed according to standard protocols. Histological examination was performed under standard microscopy.

Table I. *Summary of pancreatic cancer experimental metastasis developed from each human pancreatic cancer cell line.*

	Liver metastasis	Lung metastasis
	Number of mice with metastasis/total number of mice	
AsPC-1	3/5 (60%)	1/5 (20%)
Panc-1	1/5 (20%)	0/5 (0%)
KP2	3/5 (60%)	0/5 (0%)
KP3	1/5 (20%)	0/5 (0%)

Statistical analysis. The two-sided *t*-test was used to determine statistical significance. Differences were considered significant when the *p*-value was less than 0.05.

Results and Discussion

Establishment of pancreatic cancer experimental metastatic models. Human pancreatic cancer cell lines, AsPC-1, Panc-1, KP2, KP3, were engineered to express green fluorescent protein (GFP) (Figure 1). Each GFP-expressing pancreatic cancer cell line was injected in the spleen of five nude mice. Six weeks later, the primary tumors in the spleen and metastasis to various organs could be observed (Figures 2-5).

Metastatic characteristics of the pancreatic cancer cell lines. Each model formed primary tumors in the spleen and had a differential metastatic pattern (Table I). Three of five mice implanted with AsPC-1 and KP2 developed liver metastasis (Figure 2, Figure 4, respectively), whereas, only one mouse implanted with Panc-1 and KP3 had liver metastasis (Figure 3, Figure 5, respectively). AsPc-1- and KP2-implanted mice had approximately 30 metastases in the liver, in contrast to Panc-1- and KP3-implanted mice which had just a few metastases ($p<0.05$) (Figure 6A). Lung metastases were also observed in AsPC-1.

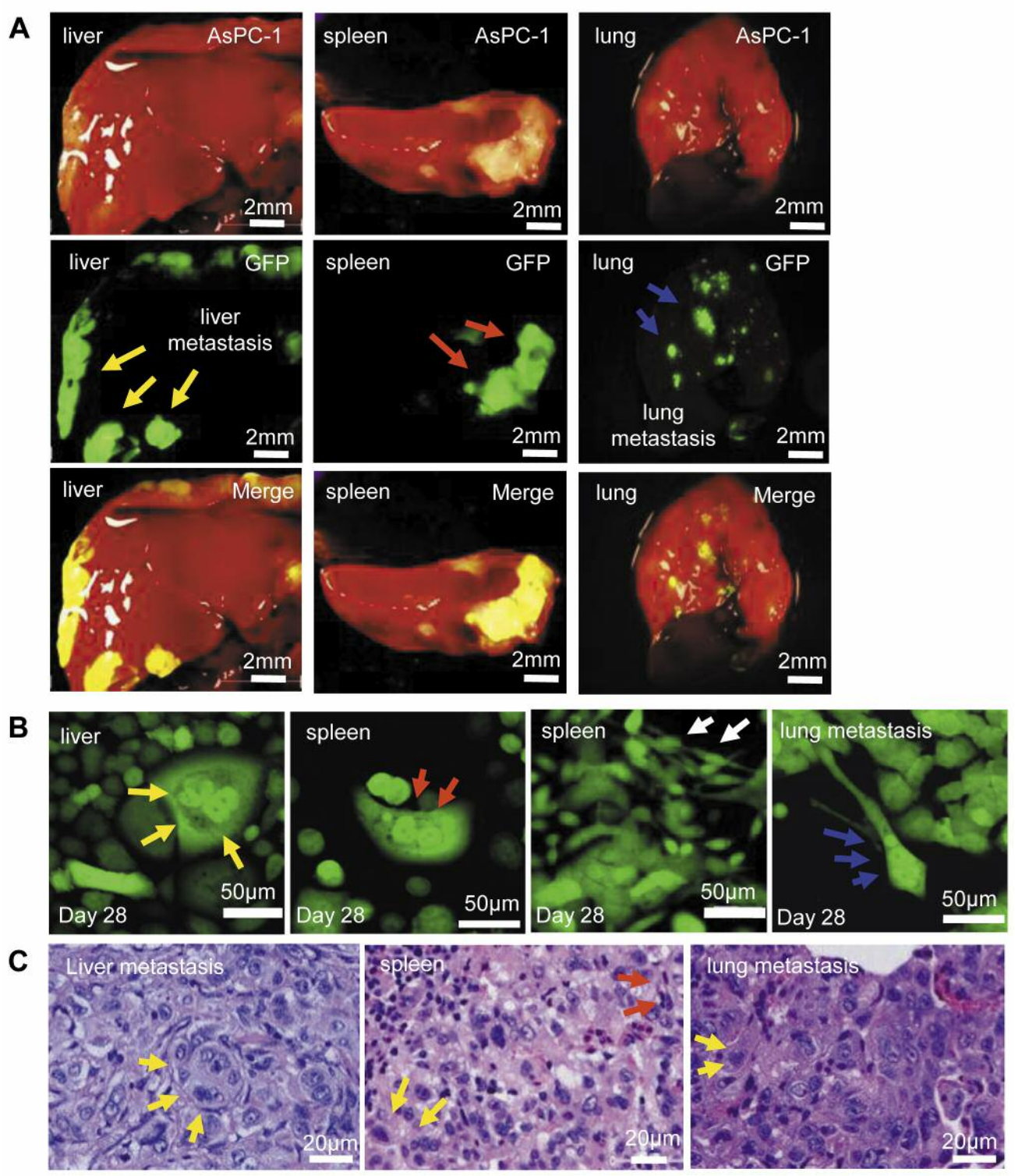

Figure 2. *AsPC-1 human pancreatic cancer experimental metastasis model. (A) Bright-field and fluorescence images of liver, spleen, and lung. Yellow arrows indicate liver metastasis. Red arrows indicate primary tumors in the spleen. Blue arrows indicate lung metastasis. Images were obtained with the SZX7 microscope. (B) High-magnification images of metastatic cells cultured from tumors in each organ. Multi-nucleate cells were cultured from the spleen (red arrows); liver (yellow arrows); lung metastasis contained spindle cells (blue arrows) as did the tumor in the spleen (white arrows). Images were obtained with the Olympus FV1000 confocal microscope. (C) Hematoxylin and eosin (H&E) stained section of AsPC-1 tumors. Yellow arrows indicate multi-nucleate cells. Red arrows indicate spindle-like cells (red arrows).*

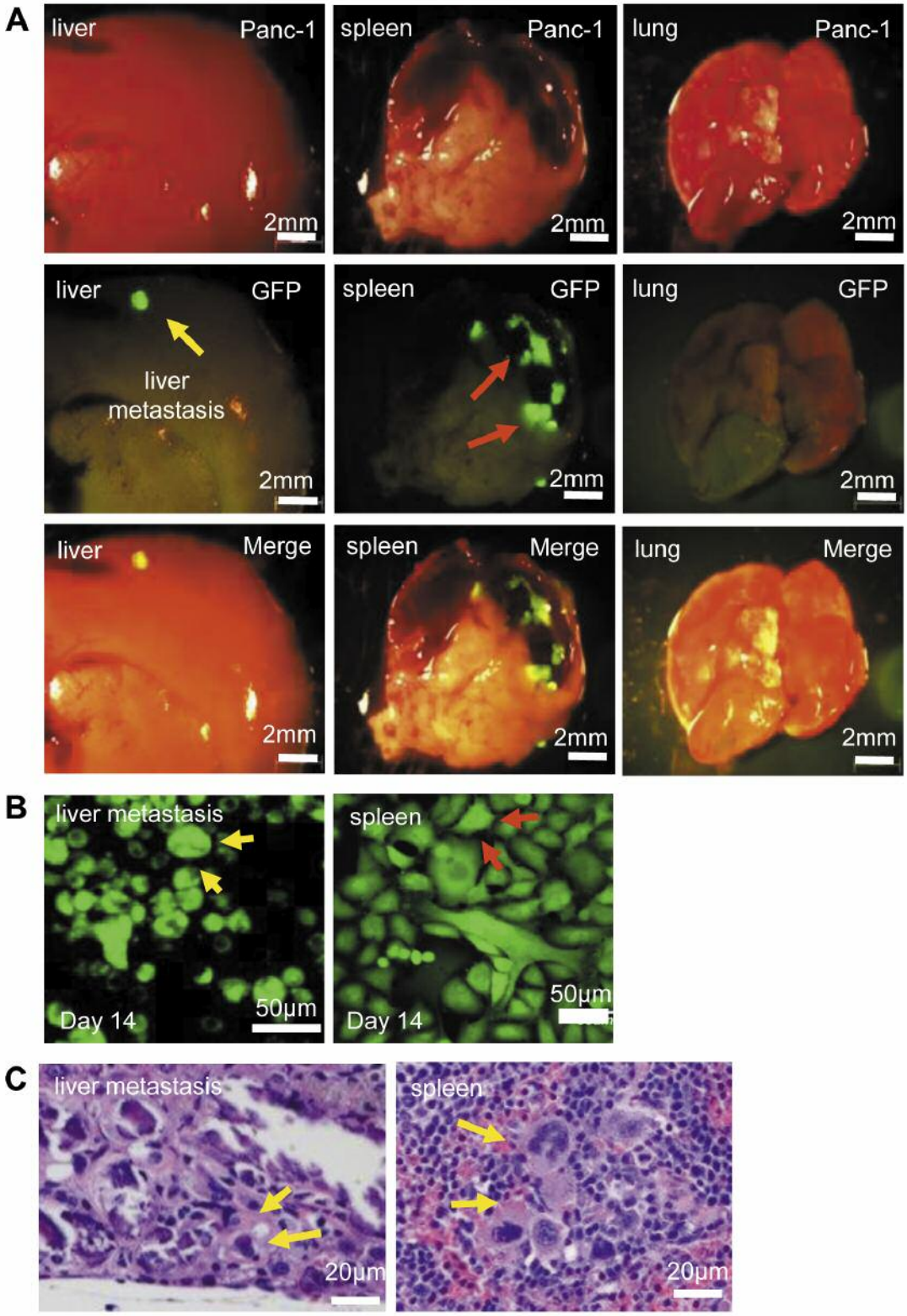

Figure 3. *Panc-1 human pancreatic cancer experimental metastasis model. (A) Bright-field and fluorescence images of liver, spleen, and lung. Red arrows indicate primary tumors. Yellow arrow indicates liver metastasis. Images were obtained with the SZX7 microscope. (B) High-magnification images of metastatic cells cultured from tumors in each organ. Multi-nucleate cells from the tumor in the spleen (red arrows) and from a liver metastasis (yellow arrows). Images were obtained with the Olympus FV1000 confocal microscope. (C) Multi-nucleate cells (yellow arrows) in H&E sections.*

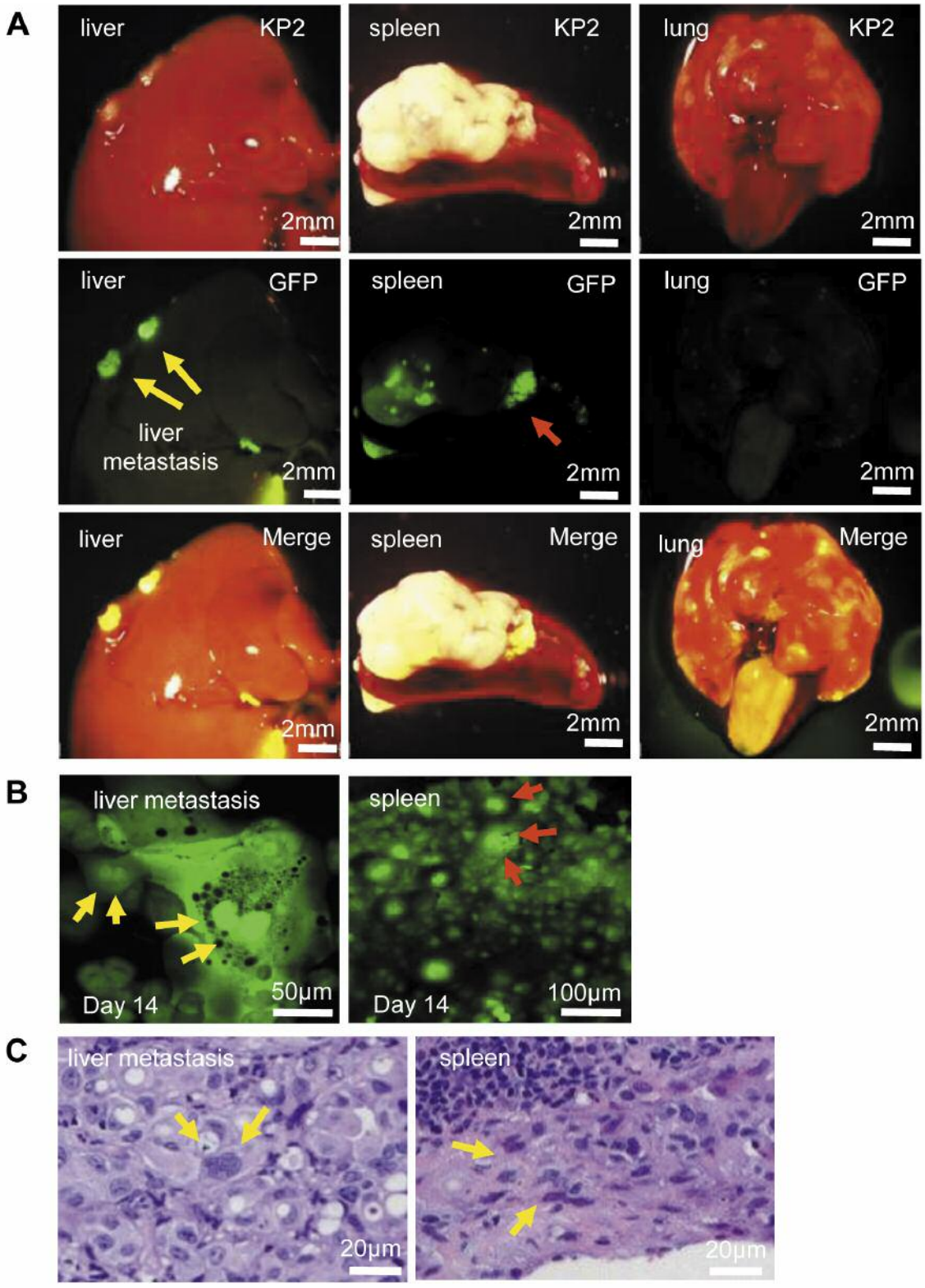

Figure 4. *KP2 human pancreatic cancer experimental metastasis model. (A) Bright-field and fluorescence images of liver, spleen, and lung. Primary tumor in the spleen (red arrow). Liver metastasis (yellow arrows). Images were obtained with the SZX7 microscope. (B) Representative images of metastatic cells, cultured from the spleen and liver metastasis. Multi-nucleate cells from liver metastasis (yellow arrows). Multi-nucleate cancer cells from the spleen (red arrows). (C) Multi-nucleate cancer cells (yellow arrows) in H&E sections.*

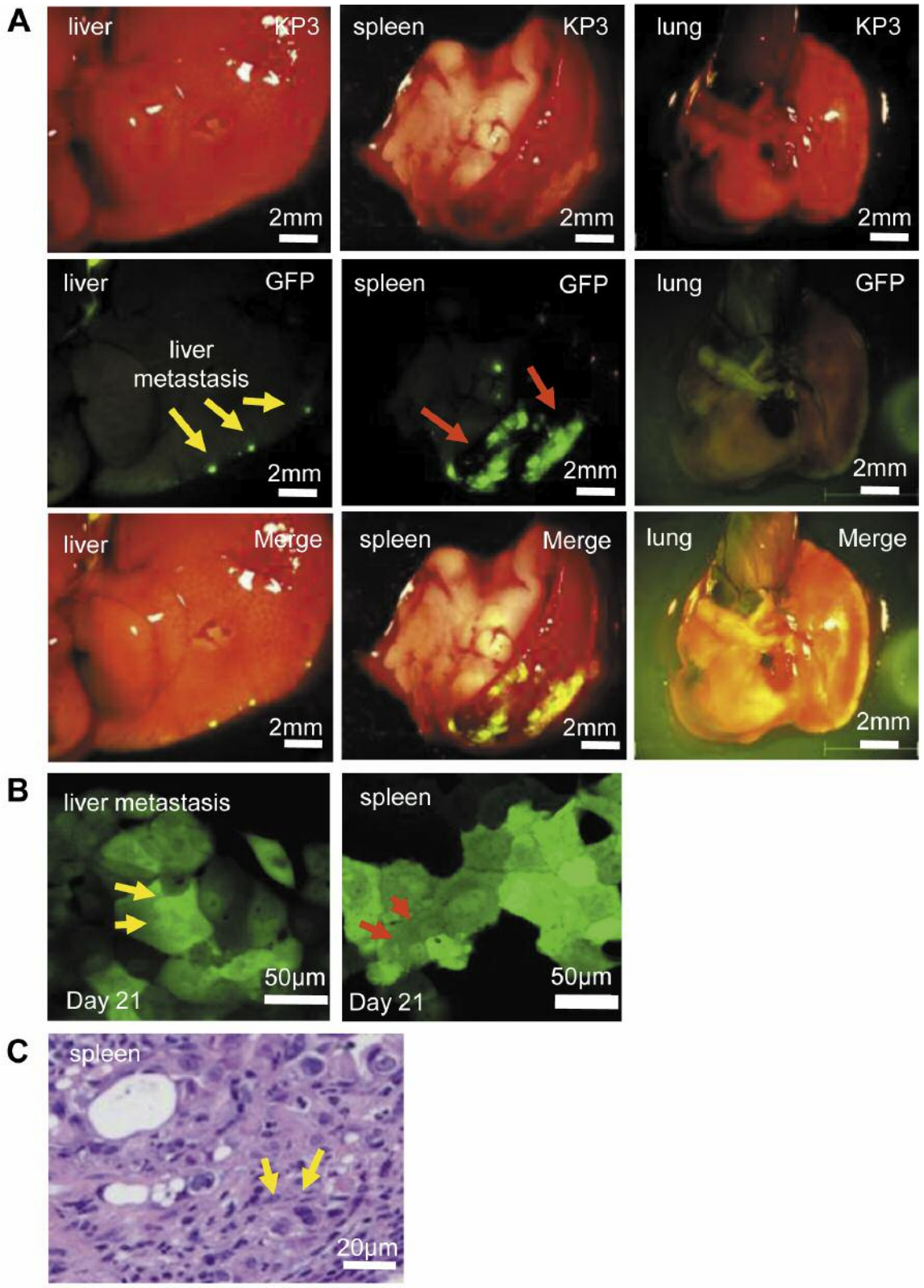

Figure 5. *KP3 human pancreatic cancer experimental metastasis model. (A) Bright-field and fluorescence images of liver, spleen, and lung. Red arrows indicate primary tumors. Yellow arrows indicate liver metastasis. (B) High magnification of multi-nucleate cells from liver metastasis (yellow arrows) and tumor in the spleen (red arrows) (Bar=50 μm). (C) Multi-nucleate cells (yellow arrows) in an H&E section.*

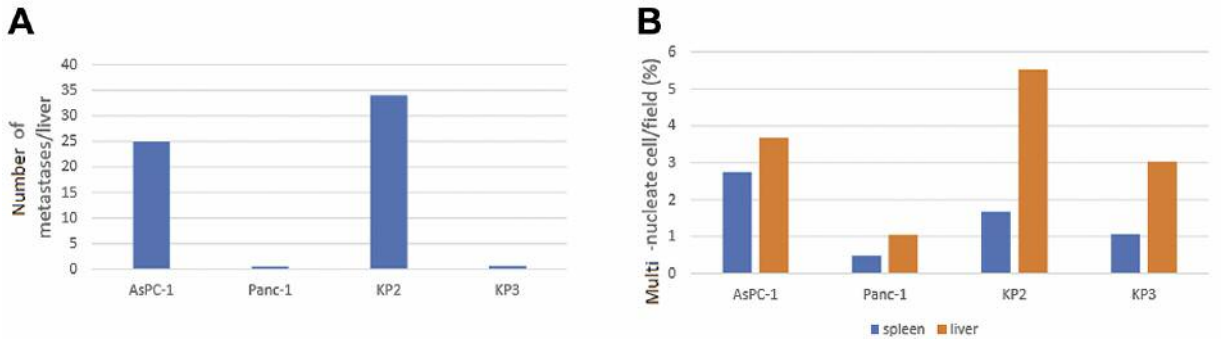

Figure 6. *(A) Bar graphs show the average number of total metastasis in the liver in mouse models for each pancreatic cancer cell line. (B) Percentage multi-nucleate cell per total cells in 5 high magnification fields in cells cultured from liver metastasis of each pancreatic cancer cells line.*

Morphology of cells cultured from primary tumors and metastases of the four human pancreatic cancer cell lines. We previously reported multi-nucleate cells were related to peritoneal metastasis of pancreatic cancer (21). In the present study, we observed multi-nucleate cells for every cell line cultured both from the primary tumor and metastatic tumors (Figures 2-5). However, there were more multi-nucleate cells in the liver metastases than in primary tumors, especially for KP2 and KP3 ($p<0.05$) (Figure 6B).

It has been reported that multi-nucleate cells were generated from cancer-cell fusion, and such fused cells may have high metastatic potential (21, 41-48). Fusion may take palce among cancer cells shed into the circulation (48, 49). The multinucleate high-metastatic cells observed in the present report may have resulted from cell fusion. Spindle cells were also frequently detected in AsPC-1, but rarely in the other cell lines. This result may suggest a relationship between spindle-like cells and lung metastasis, since only AsPC-1 formed lung metastasis. High-metastatic spindle cells that behave, as stem-like cells *in vivo*, were also previously discovered by us in a dimorphic pancreatic cancer cell line (22). Spindle-like cells may have a major functional role in the epithelial-mesenchymal transition (EMT) (28-30).

Conclusion

Each of the four human pancreatic cancer cell lines described in the present report have a characteristic pattern of metastasis. Abnormal multi-nucleate cells and spindle-like cells were more prominent in metastasis in all 4 pancreatic cancer cell lines studied. Further experiments are required to elucidate the role of multi-nucleate cells and spindle-like cells in metastasis and how they are formed and whether they are targets for anti-metastatic therapy and what is their main biochemical change (4).

Acknowledgements

This study was supported in part by Grant-in-Aid for Scientific Research (17K09457 to A.S.) from the Ministry of Education, Science, Sports and Culture of Japan.

References

1 Hidalgo M: Pancreatic cancer. N Engl J Med *362*: 1605-1617, 2010.
2 Tuveson DA and Neoptolemos JP: Understanding metastasis in pancreatic cancer: a call for new clinical approaches. Cell *148*: 21-23, 2012.
3 Fu X, Guadagni F and Hoffman RM: A metastatic nude-mouse model of human pancreatic cancer constructed orthotopically with histologically intact patient specimens. Proc Natl Acad Sci USA *89*: 5645-5649, 1992.
4 Matsuo Y, Raimondo M, Woodward TA, Wallace MB, Gill KR, Tong Z, Burdick MD, Yang Z, Strieter RM, Hoffman RM and Guha, S: CXC-chemokine/CXCR2 biological axis promotes angiogenesis *in vitro* and *in vivo* in pancreatic cancer. Int J Cancer *125*: 1027-1037, 2009.
5 Haeno H, Gonen M, Davis MB, Herman JM, Iacobuzio-Donahue CA and Michor F: Computational modeling of pancreatic cancer reveals kinetics of metastasis suggesting optimum treatment strategies. Cell *148*: 362-375, 2012.
6 Nanda S: Cancer: Pancreatic carcinomas metastasize at a late stage in their development. Nat Rev Gastroenterol Hepatol *8*: 4, 2011.
7 Chishima T, Miyagi Y, Wang X, Yamaoka H, Shimada H, Moossa AR and Hoffman RM: Cancer invasion and micrometastasis visualized in live tissue by green fluorescent protein expression. Cancer Res *57*: 2042-2047, 1997.
8 Yang M, Baranov E, Jiang P, Sun F-X, Li X-M, Li L, Hasegawa S, Bouvet M, Al-Tuwaijri M, Chishima T, Shimada H, Moossa AR, Penman S and Hoffman RM: Whole-body optical imaging of green fluorescent protein-expressing tumors and metastases. Proc Natl Acad Sci USA *97*: 1206-1211, 2000.
9 Hoffman RM and Yang M: Subcellular imaging in the live mouse. Nature Protocols *1*: 775-782, 2006.

10 Hoffman RM and Yang M: Color-coded fluorescence imaging of tumor-host interactions. Nat Protoc *1*: 928-935, 2006.
11 Hoffman RM and Yang M: Whole-body imaging with fluorescent proteins. Nature Protocols *1*: 1429-1438, 2006.
12 Suetsugu A, Osawa Y, Nagaki M, Saji S, Moriwaki H, Bouvet M and Hoffman RM: Imaging the recruitment of cancer-associated fibroblasts by liver-metastatic colon cancer. J Cell Biochem *112*: 949-953, 2011.
13 Suetsugu A, Hassanein MK, Reynoso J, Osawa Y, Nagaki M, Moriwaki H, Saji S, Bouvet M and Hoffman R.M: The cyan fluorescent protein nude mouse as a host for multicolor-coded imaging models of primary and metastatic tumor microenvironments. Anticancer Res *32*: 31-38, 2012.
14 Suetsugu A, Katz M, Fleming J, Truty M, Thomas R, Saji S, Moriwaki H, Bouvet M and Hoffman RM: Imageable fluorescent metastasis resulting in transgenic GFP mice orthotopically implanted with human-patient primary pancreatic cancer specimens. Anticancer Res *32*: 1175-1180, 2012.
15 Suetsugu A, Katz M, Fleming J, Truty M, Thomas R, Moriwaki H, Bouvet M, Saji S and Hoffman RM: Multi-color palette of fluorescent proteins for imaging the tumor microenvironment of orthotopic tumorgraft mouse models of clinical pancreatic cancer specimens. J Cell Biochem *113*: 2290-2295, 2012.
16 Suetsugu A, Katz M, Fleming J, Truty M, Thomas R, Saji S, Moriwaki H, Bouvet M and Hoffman RM: Non-invasive fluorescent-protein imaging of orthotopic pancreatic-cancer-patient tumorgraft progression in nude mice. Anticancer Res *32*: 3063-3068, 2012.
17 Matsumoto T, Suetsugu A, Shibata Y, Nakamura N, Aoki H, Kunisada T, Tsurumi H, Shimizu M and Hoffman RM: A color-coded imageable syngeneic mouse model of stromal-cell recruitment by metastatic lymphoma. Anticancer Res *35*: 4647-4654, 2015.
18 Suetsugu A, Hiroshima Y, Matsumoto T, Hasagawa K, Nakamura M, Shimizu M, Saji S, Moriwaki H, Bouvet M and Hoffman RM: Recruitment of cancer-associated fibroblasts and blood vessels by orthotopic liver tumors imaged in red fluorescent protein (RFP) transgenic nude mice. Anticancer Res *35*: 5821-5825, 2015.
19 Matsumoto T, Suetsugu A, Hasegawa K, Nakamura M, Aoki H, Kunisada T, Tsurumi H, Shimizu M and Hoffman RM: Color-coded imaging of syngeneic orthotopic malignant lymphoma interacting with host stromal cells during metastasis. Anticancer Res *36*: 1473-1478, 2016.
20 Nakamura M, Suetsugu A, Hasegawa K, Matsumoto T, Aoki H, Kunisada T, Shimizu M, Saji S, Moriwaki H and Hoffman RM: Choline-deficient-diet-induced fatty liver is a metastasis-resistant microenvironment. Anticancer Res *37*: 3429-3434, 2017.
21 Hasegawa K, Suetsugu A, Nakamura M, Matsumoto T, Aoki H, Kunisada T, Shimizu M, Saji S, Moriwaki H and Hoffman RM: Imaging the role of multinucleate pancreatic cancer cells and cancer-associated fibroblasts in peritoneal metastasis in mouse models. Anticancer Res *37*: 3435-3440, 2017.
22 Hassanein MK, Suetsugu A, Saji S, Moriwaki H, Bouvet M, Moossa AR and Hoffman RM: Stem-like and non-stem human pancreatic cancer cells distinguished by morphology and metastatic behavior. J Cell Biochem *112*: 3549-3554, 2011.
23 Rhim AD, Mirek ET, Aiello NM, Maitra A, Bailey JM, McAllister F, Reichert M, Beatty GL, Rustgi AK, Vonderheide RH, Leach SD and Stanger BZ: EMT and dissemination precede pancreatic tumor formation. Cell *148*: 349-361, 2012.
24 Suetsugu A, Snyder CS, Moriwaki H, Saji S, Bouvet M and Hoffman RM: Imaging the interaction of pancreatic cancer and stellate cells in the tumor microenvironment during metastasis. Anticancer Res *35*: 2545-2551, 2015.
25 Thiery JP, Acloque H, Huang RY and Nieto MA: Epithelial-mesenchymal transitions in development and disease. Cell *139*: 871–890, 2009.
26 Klein CA: Parallel progression of primary tumours and metastases. Nat Rev Cancer *9*: 302-312, 2009.
27 Das S and Batra SK: Pancreatic cancer metastasis: Are we being pre-EMTed? Curr Pharm Des *21*: 1249-1255, 2015.
28 Gupta S and Maitra A: EMT: matter of life or death? Cell *164*: 840-842, 2016.
29 Nieto MA, Huang RY, Jackson RA and Thiery JP: Cell *166*: 21-45, 2016.
30 Zheng X, Carstens JL, Kim J, Scheible M, Kaye J, Sugimoto H, Wu CC, LeBleu VS and Kalluri R: Epithelial-to-mesenchymal transition is dispensable for metastasis but induces chemo-resistance in pancreatic cancer. Nature *527*: 525-530, 2015.
31 Murakami T, Hiroshima Y, Zhang Y, Zhao M, Kiyuna T, Hwang HK, Miyake K, Homma Y, Mori R, Matsuyama R, Chishima T, Ichikawa Y, Tanaka K, Bouvet M, Endo I and Hoffman RM: Tumor-targeting *Salmonella typhimurium* A1-R promotes tumoricidal $CD8^+$ T cell tumor infiltration and arrests growth in a syngeneic pancreatic cancer orthotopic mouse model. J Cell Biochem *119*: 634-639, 2017.
32 Hoffman RM: The multiple uses of fluorescent proteins to visualize cancer *in vivo*. Nature Reviews Cancer *5*: 796-806, 2005.
33 Hoffman RM: Application of GFP imaging in cancer. Laboratory Investigation *95*: 432-452, 2015.
34 Hoffman RM: *In vivo* cellular imaging using fluorescent proteins. Methods and Protocols. Methods in Molecular Biology, Vol. 872, Springer Protocols, ISBN 978-1-61779-796-5, Humana Press, 2012.
35 Kawaguchi K, Igarashi K, Li S, Han Q, Tan Y, Kiyuna T, Miyake K, Murakami T, Chmielowski B, Nelson SD, Russell TA, Dry SM, Li Y, Unno M, Eilber FC and Hoffman RM: Combination treatment with recombinant methioninase enables temozolomide to arrest a BRAF V600E melanoma growth in a patient-derived orthotopic xenograft. Oncotarget *8*: 85516-85525, 2017.
36 Kawaguchi K, Igarashi K, Li S, Han Q, Tan Y, Miyake K, Kiyuna T, Miyake M, Murakami T, Chmielowski S, Nelson SD, Russell TA, Dry SM, Li Y, Unno M, Eilber FC and Hoffman RM: Recombinant methioninase (rMETase) is an effective therapeutic for BRAF-V600E-negative as well as -positive melanoma in patient-derived orthotopic xenograft (PDOX) mouse models. Oncotarget *9*: 915-923, 2018.
37 Kawaguchi K, Han Q, Li S, Tan Y, Igarashi K, Kiyuna T, Miyake K, Miyake M, Chmielowski B, Nelson SD, Russell TA, Dry SM, Li Y, Singh AS, Eckhardt MA, Unno M, Eilber FC and Hoffman RM: Targeting methionine with oral recombinant methioninase (o-rMETase) arrests a patient-derived orthotopic xenograft (PDOX) model of BRAF-V600E mutant melanoma: implications for clinical cancer therapy and prevention. Cell Cycle, 2017. doi: 10.1080/15384101.2017.1405195. [Epub ahead of print]
38 Kawaguchi K, Murakami T, Chmielowski B, Igarashi K, Kiyuna T, Unno M, Nelson SD, Russell TA, Dry SM, Li Y, Eilber FC

and Hoffman RM: Vemurafenib-resistant BRAF-V600E mutated melanoma is regressed by MEK targeting drug trametinib, but not cobimetinib in a patient-derived orthotopic xenograft (PDOX) mouse model. Oncotarget *7*: 71737-71743, 2016.

39 Kawaguchi K, Igarashi K, Murakami T, Chmielowski B, Kiyuna T, Zhao M, Zhang Y, Singh A, Unno M, Nelson SD, Russell TA, Dry SM, Li Y, Eilber FC and Hoffman RM: Tumor-targeting *Salmonella typhimurium* A1-R combined with temozolomide regresses malignant melanoma with a BRAF-V600 mutation in a patient-derived orthotopic xenograft (PDOX) model. Oncotarget *7*: 85929-85936, 2016.

40 Kawaguchi K, Igarashi K, Murakami T, Zhao M, Zhang Y, Chmielowski B, Kiyuna T, Nelson SD, Russell TA, Dry SM, Li Y, Unno M, Eilber FC and Hoffman RM: Tumor-targeting *Salmonella typhimurium* A1-R sensitizes melanoma with a BRAF-V600E mutation to vemurafenib in a patient-derived orthotopic xenograft (PDOX) nude mouse model. J Cell Biochem *118*: 2314-2319, 2017.

41 Duelli D and Lazebnik Y: Cell fusion: a hidden enemy? Cancer Cell *3*: 445-448, 2003.

42 Lu X and Kang Y: Cell fusion as a hidden force in tumor progression. Cancer Res *69*: 8536-8539, 2009.

43 Lu X and Kang Y: Efficient acquisition of dual metastasis organotropism to bone and lung through stable spontaneous fusion between MDA-MB-231 variants. Proc Natl Acad Sci USA *106*: 9385-9390, 2009.

44 Fortuna MB, Dewey MJ and Furmanski P: Cell fusion in tumor development and progression: occurrence of cell fusion in primary methylcholantrene-induced tumorigenesis. Int J Cancer *44*: 731-737, 1989.

45 Seyfried TN and Huysentruyt LC: On the origin of cancer metastasis. Crit Rev Oncog *18*: 43-73, 2013.

46 Zhang S, Mercado-Uribe I, Xing Z, Sun B, Kuang J and Liu J: Generation of cancer stem-like cells through the formation of polyploid giant cancer cells. Oncogene *33*: 116-128, 2014.

47 Nakamura M, Suetsugu A, Hasegawa K, Matsumoto T, Aoki H, Kunisada T, Shimizu M, Saji S, Moriwaki H and Hoffman RM: Genetic recombination between stromal and cancer cells results in highly malignant cells identified by color-coded imaging in a mouse lymphoma model. J Cell Biochem *118*: 4216-4221, 2017.

48 Glinsky GV, Glinskii AB, Berezovskaya O, Smith BA, Jiang P, Li X-M, Yang M and Hoffman RM: Dual-color-coded imaging of viable circulating prostate carcinoma cells reveals genetic exchange between tumor cells *in vivo*, contributing to highly metastatic phenotypes. Cell Cycle *5*: 191-197, 2006.

49 Glinskii AB, Smith BA, Jiang P, Li X-M, Yang M, Hoffman RM and Glinsky GV: Viable circulating metastatic cells produced in orthotopic but not ectopic prostate cancer models. Cancer Res *63*: 4239-4243, 2003.

Received January 24, 2018
Revised February 16, 2018
Accepted February 20, 2018